Nov 9th, 12:00 AM - 12:00 AM

Numerical Simulations of Solid and Slotted Cold-Formed Steel Channels with Different Boundary Conditions in Shear

Vitaliy V. Degtyarev

Natalia V. Degtyareva

Wei-Wen Yu International Specialty Conference on Cold-Formed Steel Structures
Baltimore, Maryland, U.S.A, November 9 & 10, 2016

Numerical Simulations of Solid and Slotted Cold-Formed Steel Channels with Different Boundary Conditions in Shear

Vitaliy V. Degtyarev[1] and Natalia V. Degtyareva[2]

Abstract

This paper presents results of a numerical study on the shear strength of cold-formed steel channels with solid and slotted webs. The effects of four different boundary conditions—test setup, realistic, and simply supported with free and restrained ends—on the elastic shear buckling load and the ultimate shear strength were considered. The study was performed on finite element models developed in ANSYS and validated against test data. The obtained results showed that the elastic shear buckling loads and the ultimate shear strengths of the slotted channels are more sensitive to the boundary conditions when compared with the solid channels. The simply supported boundary conditions can reasonably well simulate the test setup boundary conditions of the solid channels but not the slotted channels. The realistic boundary conditions cannot be accurately simulated by the simply supported boundary conditions for the solid and slotted channels.

Introduction

Cold-formed steel (CFS) studs and purlins with slotted webs have been developed and used to reduce thermal bridging and to make the CFS framing thermally efficient (AISI/Steel Framing Alliance 2002b, Höglund and Burstrand 1998, and Liptak-Varadi 2010). AISI/Steel Framing Alliance (2002a), Kesti (2000), and Salhab and Wang (2008) studied the effects of the slotted webs on the strength and behavior of CFS channels in compression and bending.

Degtyareva and Degtyarev (2016) experimentally investigated the shear strength of the slotted channels and found that the ultimate shear strength was greatly affected by web perforations. Tentative equations for the shear capacity

[1] Design Engineer, New Millennium Building Systems, Columbia, SC, USA
[2] Associate Professor, South Ural State University, Chelyabinsk, Russia

of the slotted channels with and without tension field action were proposed. The proposed equations can only be used for the channels with the perforation pattern tested in the study. Additional investigations are required to determine the effects of different slot sizes and patterns on the shear strength of CFS channels.

Keerthan and Mahendran (2010b, 2015), LaBoube and Yu (1978), and Pham and Hancock (2012) demonstrated that the ultimate shear strength of CFS channels with solid webs depended on the test setup and support conditions. Based on results of numerical simulations, Degtyarev and Degtyareva (2016) showed that the shear strength of the slotted channels is more affected by the boundary conditions than the strength of the solid channels.

The objectives of this study were to numerically investigate the effects of different boundary conditions on the elastic shear buckling load and the ultimate shear strength of CFS channels with solid and slotted webs and to determine whether or not simplified boundary conditions can simulate the test setup and realistic boundary conditions with acceptable accuracy. The simplified boundary conditions are attractive for the use in numerical parametric studies because they can be modeled more easily than the tests setup and realistic boundary conditions.

The study by Degtyarev and Degtyareva (2016) was expanded in this work to include solid and slotted CFS channels with simply supported boundary conditions. Two simply supported boundary conditions were considered: with coupled and with uncoupled translations of the nodes at the supported web edge in the direction parallel to the channel length. Those boundary conditions are referenced in this paper as simply supported boundary conditions with the restrained and free ends, respectively.

The studies were performed on non-linear finite element (FE) models developed in ANSYS and validated against test data. The FE method has proven to be an effective and powerful tool for analysis of CFS members in shear and for predicting their shear strength and behavior (Degtyarev and Degtyareva 2016, Keerthan and Mahendran 2010a, 2011a, 2011b, 2013a, 2013b, 2014, and 2015, Pham and Hancock 2010, 2012, and 2015, and Pham et al. 2014).

Numerical study program

The CFS channels with solid and slotted webs experimentally studied by Degtyareva and Degtyarev (2016) were modeled in ANSYS. The tested

profiles are shown in Fig. 1. Actual properties of the tested channels can be found in Degtyareva and Degtyarev (2016).

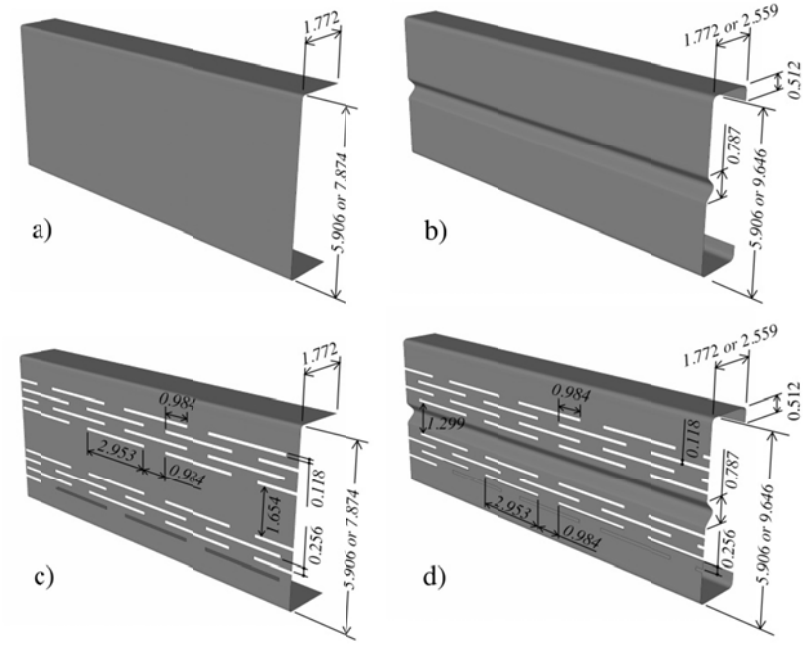

Fig. 1. Tested and modeled profiles (nominal dimensions in inches are shown): a) and b) channels with solid unstiffened and stiffened webs; c) and d) channels with slotted unstiffened and stiffened webs

The test specimens consisted of two identical channels bolted back-to-back. Flanges of some of the channels were reinforced with steel plates to prevent the specimen failure in bending and combined bending and shear. Due to the symmetry, only one-half of one channel and web side plates (WSP) on only one side were modeled. The four-node elements with six degrees of freedom at each node, type SHELL181, were used for the CFS channels, reinforcing plates and WSPs.

The bilinear isotropic hardening material model (BISO) was used for the channels and the reinforcing plates, which were assumed to be elastic-perfectly plastic. The WSPs were modeled as elastic shell elements. The elastic modulus and Poisson's ratio were taken as 29008 ksi (200,000 MPa) and 0.3, respectively, for all model components. Screw connections between the

reinforcing plates and the channels were modeled with COMBIN39 nonlinear spring elements in the longitudinal direction, which allowed for taking the connections flexibility into consideration. The force-deflection behavior of the COMBIN39 elements was elastic for the forces up to the screw strength and perfectly plastic beyond the deflection corresponding to the screw strength. The AISI S310 (2013) equations were used to determine the shear strength and flexibility of the screws.

All model components were discretized with quadrilateral element meshes. Based on the convergence study described in Degtyarev and Degtyareva (2016), the maximum element size of 0.197 in. (5 mm) was selected for the solid channels. The non-perforated regions of the slotted channels and their perforated regions in the longitudinal direction were also meshed using the maximum element size of 0.197 in. (5 mm). The perforated regions in the vertical direction were meshed using the maximum element size of 0.059 in. (1.5 mm).

Four different boundary conditions were considered: test setup, realistic, simply supported with the free end, and simply supported with the restrained end. A detailed description of the modeled test setup and realistic boundary conditions can be found in Degtyarev and Degtyareva (2016). The simplified boundary conditions are shown in Fig. 2.

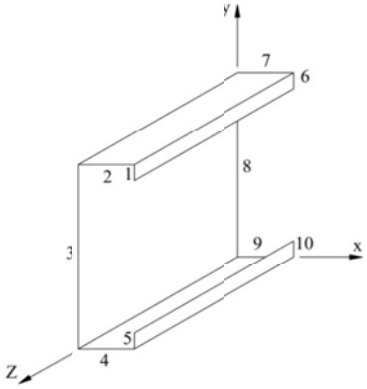

Edges	*u*	*v*	*w*
1 2 4 5	0	0	1
3	1	0	1
6 7 9 10	0	0	0
8	1	1	0

Notes:
1) *u*, *v* and *w* are translations in the *x*, *y* and *z* directions, respectively. 0 denotes free and 1 denotes restrained degree of freedom.
2) in simply supported boundary conditions with the restrained end, translations of edge 8 nodes in the *z* direction were coupled.

Fig. 2. Simplified boundary conditions

The models were loaded by an imposed displacement applied in small increments to one of the nodes at the WSP edge (for the test setup boundary conditions) or to one of the nodes at the left channel edge (edge 3 in Fig. 2; for the realistic and simplified boundary conditions).Vertical translations of the nodes at edge 3 were coupled in the models with the realistic and simplified

boundary conditions. The initial geometric imperfection of $h/150$ was used (Degtyarev and Degtyareva 2016).

The FE analysis was performed in two steps. First, the elastic buckling analysis was run to obtain the elastic shear buckling loads and modes. Afterwards, the nonlinear static analysis was performed to obtain the ultimate shear strength and the failure mode of the model. The lowest elastic shear buckling mode was used in the nonlinear analysis for modeling the initial geometric imperfections. The effects of large deformations and material yielding were taken into consideration in the nonlinear analysis. The L2-norm (square root sum of the squares) with the tolerance values of 0.05 and 0.005 for moments and forces, respectively, was used for the convergence criterion. The sparse direct equation solver and the automatic load stepping were specified.

A detailed validation of the developed FE models with the test setup boundary conditions against the test data is presented in Degtyarev and Degtyareva (2016). Good agreements between the experimental and simulated ultimate shear strengths can also be seen in Table 1.

Numerical simulations results and discussion

Elastic shear buckling load

Table 2 shows the elastic shear buckling loads of the analyzed channels with different boundary conditions obtained from the FE analyses. Typical lowest buckling modes of the solid and slotted channels are shown in Figs. 3 and 4, respectively.

For the slotted channels, the $V_{cr\text{-}TS}/V_{cr\text{-}R}$ ratios ranged from 1.04 to 2.07 with a mean value of 1.52 and a coefficient of variation of 0.233, which indicates that the realistic boundary conditions resulted in smaller elastic shear buckling loads when compared with those for the test setup boundary conditions. The difference in the elastic shear buckling loads increased as the web slenderness increased. These results show that the realistic boundary conditions do not provide the same restraint for the slotted channels as the test setup boundary conditions.

For the solid channels, the $V_{cr\text{-}TS}/V_{cr\text{-}R}$ ratios ranged from 0.70 to 1.49 with a mean value of 1.01 and a coefficient of variation of 0.286. In other words, the elastic shear buckling loads of solid channels with the test setup boundary conditions were either higher or smaller than those for the solid channels with the realistic boundary conditions depending on the web slenderness. On

average, the elastic shear buckling loads of the studied solid channels with both boundary conditions were approximately the same. The obtained results show that the elastic shear buckling loads of the solid channels are less sensitive to the change in the boundary conditions when compared with the slotted channels.

Table 1
Experimental and calculated ultimate shear capacities of solid and slotted channels

Specimen	V_{test} (kip)	$V_{FEA\text{-}TS}$ (kip)	$V_{FEA\text{-}R}$ (kip)	$V_{FEA\text{-}SF}$ (kip)	$V_{FEA\text{-}SR}$ (kip)	$V_{test}/V_{FEA\text{-}TS}$	$V_{FEA\text{-}TS}/V_{FEA\text{-}SF}$	$V_{FEA\text{-}TS}/V_{FEA\text{-}SR}$	$V_{FEA\text{-}R}/V_{FEA\text{-}SF}$	$V_{FEA\text{-}R}/V_{FEA\text{-}SR}$
C-150-0.9-1	2.579	2.574	2.298	2.529	3.111	1.00	1.02	0.83	0.91	0.74
C-150-0.9-2	2.534	2.624	2.246	2.525	3.116	0.97	1.04	0.84	0.89	0.72
C-150-1.5-1	6.708	7.126	7.270	6.623	7.450	0.94	1.08	0.96	1.10	0.98
C-150-1.5-2	5.706	6.866	7.264	6.598	7.430	0.83	1.04	0.92	1.10	0.98
C-200-0.9-1	2.241	2.428	2.754	2.531	3.019	0.92	0.96	0.80	1.09	0.91
C-200-1.5-1	6.666	7.115	7.951	6.596	7.565	0.94	1.08	0.94	1.21	1.05
C-200-1.5-2	6.202	7.736	7.866	6.911	7.951	0.80	1.12	0.97	1.14	0.99
CS-150-1.5-1	7.259	7.626	7.117	6.879	7.727	0.95	1.11	0.99	1.03	0.92
CS-150-2-1	9.930	11.443	9.932	10.274	11.270	0.87	1.11	1.02	0.97	0.88
CS-245-1.5-2	8.813	9.822	8.140	8.304	10.031	0.90	1.18	0.98	0.98	0.81
PC-150-0.9-1	1.014	0.969	0.753	0.553	1.144	1.05	1.75	0.85	1.36	0.66
PC-150-0.9-2	0.928	0.895	0.753	0.515	1.054	1.04	1.74	0.85	1.46	0.71
PC-150-1.5-1	1.994	1.828	1.407	1.189	2.221	1.09	1.54	0.82	1.18	0.63
PC-150-1.5-2	1.558	1.720	1.441	1.104	2.012	0.91	1.56	0.85	1.31	0.72
PC-200-0.9-1	1.129	1.322	0.883	0.663	1.167	0.85	1.99	1.13	1.33	0.76
PC-200-0.9-2	0.863	1.054	0.767	0.486	0.917	0.82	2.17	1.15	1.58	0.84
PC-200-1.5-1	2.758	2.983	2.271	1.481	2.727	0.93	2.01	1.09	1.53	0.83
PC-200-1.5-2	2.419	2.810	1.673	1.544	2.756	0.86	1.82	1.02	1.08	0.61
PCS-150-1.5-1	2.169	2.219	1.583	1.308	2.048	0.98	1.69	1.08	1.21	0.77
PCS-150-1.5-2	1.888	2.120	1.349	1.209	1.868	0.89	1.75	1.13	1.11	0.72
PCS-150-2-1	2.853	3.392	2.426	2.187	3.172	0.84	1.55	1.07	1.11	0.76
PCS-150-2-2	2.743	3.170	2.017	1.987	2.752	0.87	1.59	1.15	1.01	0.73
PCS-245-1.5-1	3.811	3.995	3.275	2.979	3.993	0.95	1.34	1.00	1.10	0.82
PCS-245-1.5-2	3.415	3.846	2.772	2.648	3.482	0.89	1.45	1.10	1.05	0.80
PCS-245-2-1	4.159	3.968	2.646	2.806	3.628	1.05	1.41	1.09	0.94	0.73
				All channels	MIN	0.80	0.96	0.80	0.89	0.61
					MAX	1.09	2.17	1.15	1.58	1.05
					MEAN	0.93	1.45	0.99	1.15	0.80
					COV	0.084	0.249	0.117	0.162	0.145
				Solid channels	MIN	0.80	0.96	0.80	0.89	0.72
					MAX	1.00	1.18	1.02	1.21	1.05
					MEAN	0.91	1.07	0.92	1.04	0.90
					COV	0.068	0.058	0.080	0.099	0.123
				Slotted channels	MIN	0.82	1.34	0.82	0.94	0.61
					MAX	1.09	2.17	1.15	1.58	0.84
					MEAN	0.93	1.69	1.03	1.23	0.74
					COV	0.093	0.140	0.119	0.159	0.093

Specimen label: *W-D-T-N*, where *W* = channel web type (*C* = solid unstiffened web, *CS* = solid stiffened web, *PC* = perforated unstiffened web, *PCS* = perforated stiffened web); *D* = nominal channel depth in mm (150, 200, and 245); *T* = nominal base steel thickness of channel in mm (0.9, 1.5, and 2); and *N* = specimen number.

Table 2
Calculated elastic shear buckling loads of solid and slotted channels

Specimen	$V_{cr\text{-}TS}$ (kip)	$V_{cr\text{-}R}$ (kip)	$V_{cr\text{-}SF}$ (kip)	$V_{cr\text{-}SR}$ (kip)	$V_{cr\text{-}TS}/V_{cr\text{-}R}$	$V_{cr\text{-}TS}/V_{cr\text{-}SF}$	$V_{cr\text{-}TS}/V_{cr\text{-}SR}$	$V_{cr\text{-}R}/V_{cr\text{-}SF}$	$V_{cr\text{-}R}/V_{cr\text{-}SR}$
C-150-0.9-1	1.920	1.306	1.659	1.767	1.47	1.16	1.09	0.79	0.74
C-150-0.9-2	1.933	1.295	1.664	1.767	1.49	1.16	1.09	0.78	0.73
C-150-1.5-1	7.756	8.282	6.825	7.273	0.94	1.14	1.07	1.21	1.14
C-150-1.5-2	7.623	8.248	6.756	7.250	0.92	1.13	1.05	1.22	1.14
C-200-0.9-1	1.045	0.818	0.944	0.996	1.28	1.11	1.05	0.87	0.82
C-200-1.5-1	5.130	5.883	4.804	4.984	0.87	1.07	1.03	1.22	1.18
C-200-1.5-2	5.546	6.519	5.123	5.350	0.85	1.08	1.04	1.27	1.22
CS-150-1.5-1	17.719	25.273	16.937	17.701	0.70	1.05	1.00	1.49	1.43
CS-150-2-1	42.934	55.793	40.533	42.568	0.77	1.06	1.01	1.38	1.31
CS-245-1.5-2	10.200	12.077	9.775	11.425	0.84	1.04	0.89	1.24	1.06
PC-150-0.9-1	0.540	0.261	0.407	0.443	2.07	1.32	1.21	0.64	0.59
PC-150-0.9-2	0.474	0.250	0.384	0.420	1.90	1.23	1.13	0.65	0.59
PC-150-1.5-1	2.127	1.585	1.659	1.783	1.34	1.28	1.19	0.96	0.89
PC-150-1.5-2	1.891	1.571	1.571	1.695	1.20	1.20	1.12	1.00	0.93
PC-200-0.9-1	0.481	0.238	0.353	0.414	2.01	1.36	1.16	0.68	0.58
PC-200-0.9-2	0.346	0.211	0.283	0.337	1.63	1.22	1.03	0.75	0.63
PC-200-1.5-1	2.232	1.565	1.632	1.958	1.43	1.37	1.14	0.96	0.80
PC-200-1.5-2	2.010	1.342	1.803	2.014	1.50	1.12	1.00	0.75	0.67
PCS-150-1.5-1	1.891	1.637	1.464	2.127	1.16	1.29	0.89	1.12	0.77
PCS-150-1.5-2	1.677	1.522	1.493	2.124	1.10	1.12	0.79	1.02	0.72
PCS-150-2-1	5.681	5.146	4.422	6.481	1.10	1.28	0.88	1.16	0.79
PCS-150-2-2	4.905	4.707	4.483	6.423	1.04	1.09	0.76	1.05	0.73
PCS-245-1.5-1	3.264	1.796	2.480	2.266	1.82	1.32	1.44	0.72	0.79
PCS-245-1.5-2	2.884	1.578	2.468	2.275	1.83	1.17	1.27	0.64	0.69
PCS-245-2-1	6.715	3.912	5.991	5.535	1.72	1.12	1.21	0.65	0.71
			All channels	MIN	0.70	1.04	0.76	0.64	0.58
				MAX	2.07	1.37	1.44	1.49	1.43
				MEAN	1.32	1.18	1.06	0.97	0.87
				COV	0.312	0.086	0.142	0.267	0.280
			Solid channels	MIN	0.70	1.04	0.89	0.78	0.73
				MAX	1.49	1.16	1.09	1.49	1.43
				MEAN	1.01	1.10	1.03	1.15	1.08
				COV	0.286	0.041	0.056	0.217	0.222
			Slotted channels	MIN	1.04	1.09	0.76	0.64	0.58
				MAX	2.07	1.37	1.44	1.16	0.93
				MEAN	1.52	1.23	1.08	0.85	0.73
				COV	0.233	0.075	0.175	0.227	0.146

For the solid and slotted channels, the simply supported boundary conditions with the free end resulted in smaller elastic shear buckling loads when compared with those for the test setup boundary conditions. The mean value of the $V_{cr\text{-}TS}/V_{cr\text{-}SF}$ ratios and their coefficient of variation were smaller for the solid channels (1.10 and 0.041 for the solid channels vs. 1.23 and 0.075 for the slotted channels). These results indicate that the simply supported boundary conditions

with the free end underestimate the restraint achieved in a typical test setup with a greater underestimation for the slotted channels.

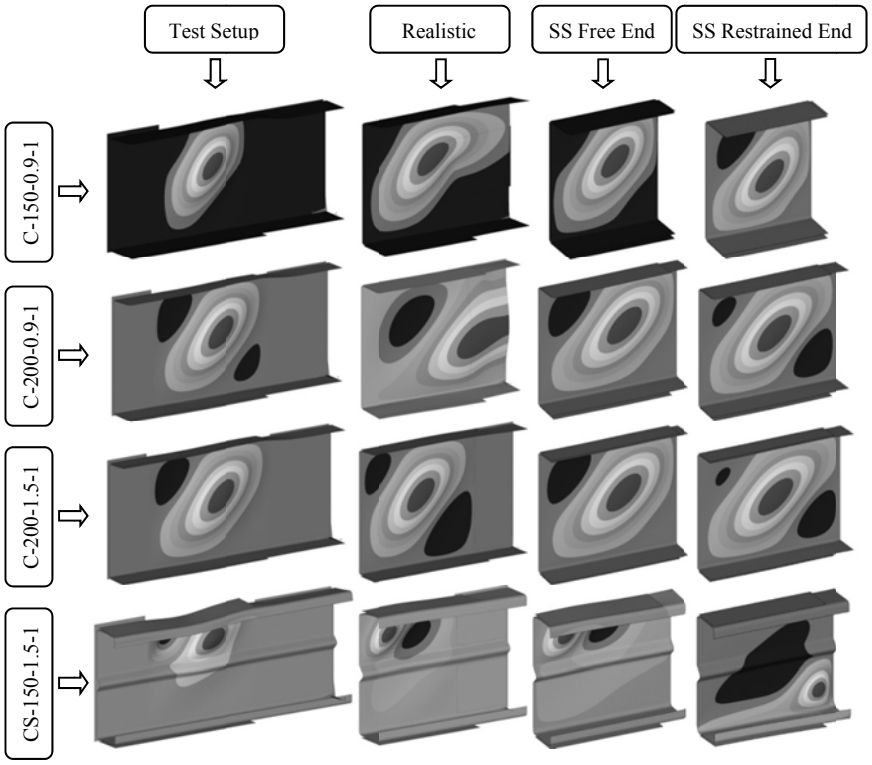

Fig. 3. Buckling modes of solid channels with different boundary conditions (SS = Simply Supported)

The simply supported boundary conditions with the restrained end resulted in better predictions of the elastic shear buckling loads of the channels with the test setup boundary conditions when compared with the simply supported boundary conditions with the free end. The mean values and the coefficients of variation of the $V_{cr\text{-}TS}/V_{cr\text{-}SR}$ ratios were 1.03 and 0.056 for the solid channels and 1.08 and 0.175 for the slotted channels. This shows that the simply supported boundary conditions with the restrained end predicted the elastic shear buckling loads of the solid channels with the test setup boundary conditions very well. For the slotted channels, the mean value of the $V_{cr\text{-}TS}/V_{cr\text{-}SR}$ ratios was close to unity but their coefficient of variation was relatively large, which does not allow us to

recommend the use of the simply supported boundary conditions for predicting the elastic shear buckling loads of the slotted channels with the test setup boundary conditions.

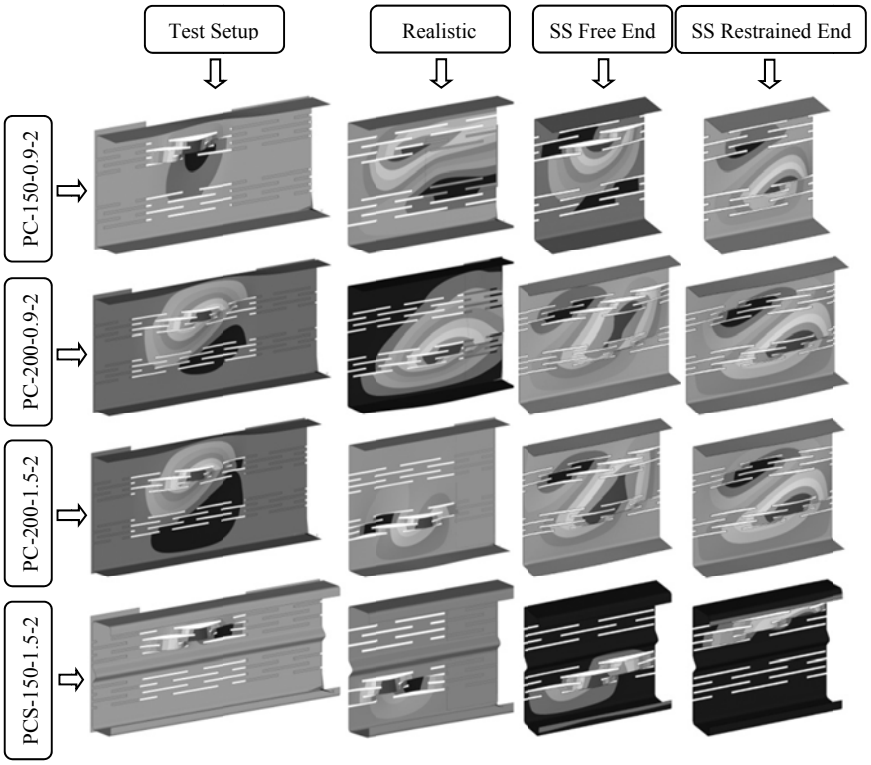

Fig. 4. Buckling modes of slotted channels with different boundary conditions (SS = Simply Supported)

The mean values and the coefficients of variations of the $V_{cr\text{-}R}/V_{cr\text{-}SF}$ ratios were 1.15 and 0.217 for the solid channels and 0.85 and 0.227 for the slotted channels. This indicates that the simply supported boundary conditions with the free end resulted, on average, in underestimated and overestimated elastic shear buckling loads for the solid and slotted channels, respectively, with the realistic boundary conditions. The coefficients of variations of the $V_{cr\text{-}R}/V_{cr\text{-}SF}$ ratios were relatively high.

The mean values and the coefficients of variation of the $V_{cr\text{-}R}/V_{cr\text{-}SR}$ ratios were 1.08 and 0.222 for the solid channels and 0.73 and 0.146 for the slotted channels. These results are similar to those for the simplified boundary conditions with the free end. The additional restraint at the channel end caused an increase in the elastic shear buckling loads. The mean value of the $V_{cr\text{-}R}/V_{cr\text{-}SR}$ ratios was close to unity for the solid channels but their coefficient of variation was relatively high.

The obtained results demonstrate that analyses with the simplified boundary conditions cannot accurately predict the elastic shear buckling loads of the slotted channels with the test setup and realistic boundary conditions. The simply supported boundary conditions with the restrained end appear to be capable of simulating the test setup boundary conditions of the solid channels for the purpose of determining the elastic shear buckling load.

The buckling modes of the solid unstiffened channels with the test setup and simply supported boundary conditions were typical for the shear loading (see Fig. 3). In the solid stiffened channels, only one vertical flat portion of the web buckled. The slender solid webs of the channels with the realistic boundary conditions buckled in a combination of shear buckling and web crippling, which caused reductions in the elastic shear buckling loads. The stocky webs demonstrated shear buckling only.

The lowest buckling mode of the slotted channels with the test setup and simply supported boundary conditions was local buckling of the channel web near the slots within the shear span (see Fig. 4). For the realistic boundary conditions, the slotted channels with slender webs demonstrated a combination of local buckling within the shear span and web crippling at the support, whereas the slotted channels with stocky webs buckled locally near the holes within the shear span similarly to the slotted channels with the test setup and simply supported boundary conditions.

Ultimate shear strength

The ultimate shear strengths of the analyzed channels with different boundary conditions are given in Table 1. Figures 5 and 6 show von Mises stresses in the solid and slotted channels, respectively, at the maximum applied load. As was discussed in Degtyarev and Degtyareva (2016), the realistic boundary conditions resulted in a relatively small (4% on average) reduction in the ultimate shear strengths of the solid channels when compared with the test setup boundary conditions. The ultimate shear strengths of the slotted channels reduced significantly more (39% on average) when the boundary conditions

changed from test setup to realistic. This shows that the ultimate shear strength of the slotted channels is more sensitive to the boundary conditions.

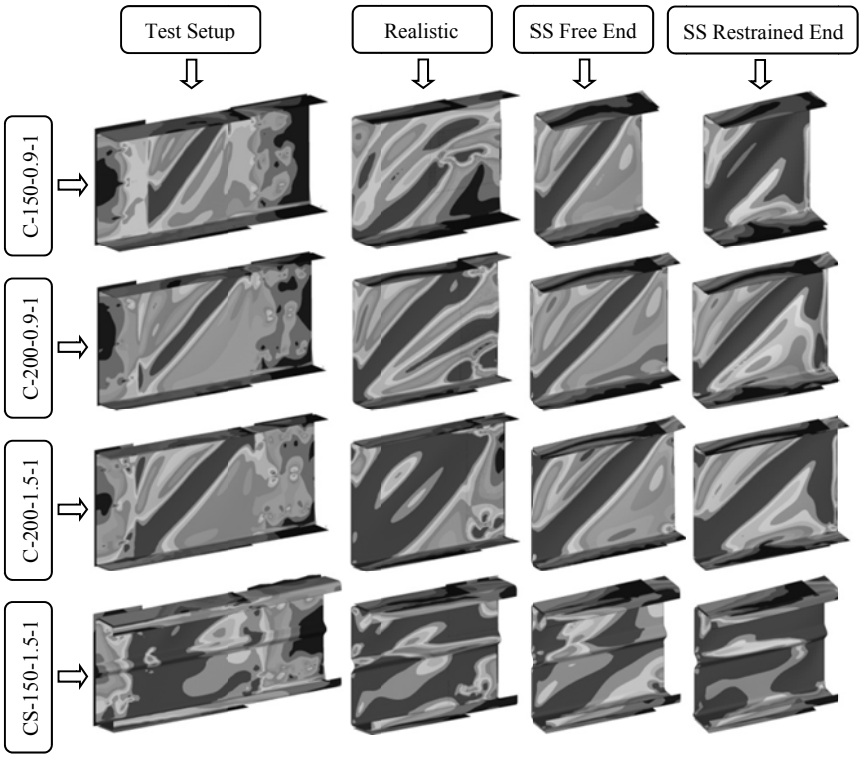

Fig. 5. Von Mises stresses in solid channels with different boundary conditions (SS = Simply Supported)

The mean values and the coefficients of variations of the $V_{FEA\text{-}TS}/V_{FEA\text{-}SF}$ and $V_{FEA\text{-}TS}/V_{FEA\text{-}SR}$ ratios for the solid channels were 1.07 and 0.058 and 0.92 and 0.080, respectively. These results show that the average ultimate shear strength of the solid channels with the test setup boundary conditions was slightly larger and slightly smaller than the strengths of the simply supported channels with the free and restrained ends, respectively.

Similarly to the test setup boundary conditions, the average ultimate shear strength of the solid channels with the realistic boundary conditions was close

to the average strengths of the simply supported solid channels. The mean values of the V_{FEA-R}/V_{FEA-SF} and the V_{FEA-R}/V_{FEA-SR} ratios were 1.04 and 0.90 for the simply supported boundary conditions with the free and restrained ends, respectively. However, their coefficients of variation were relatively high (0.099 and 0.123, respectively) and noticeably larger than those for the V_{FEA-TS}/V_{FEA-SF} and the V_{FEA-TS}/V_{FEA-SR} ratios.

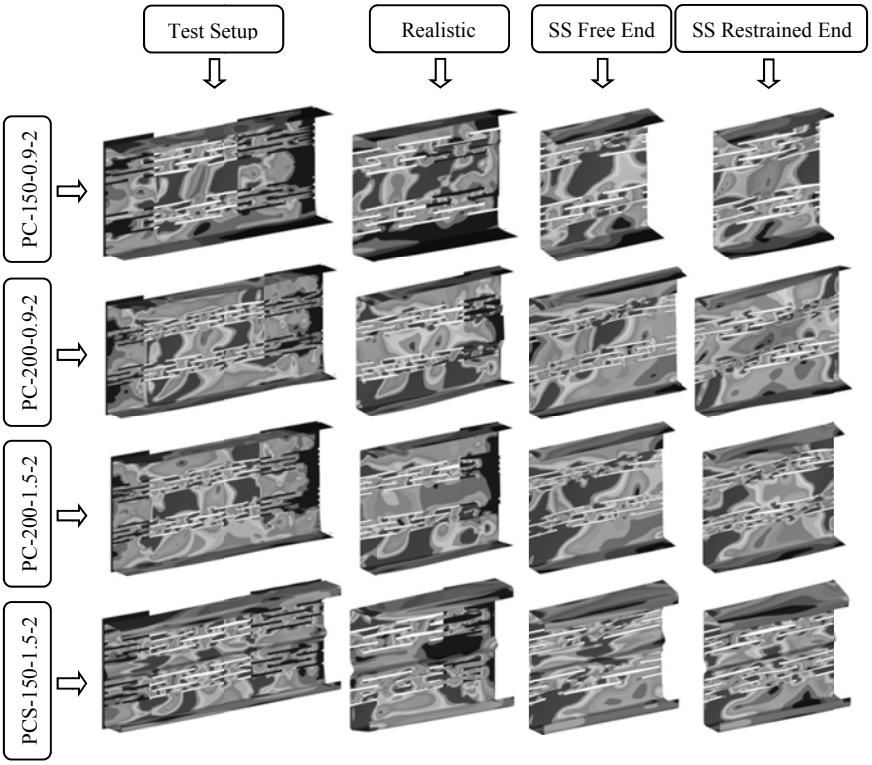

Fig. 6. Von Mises stresses in slotted channels with different boundary conditions (SS = Simply Supported)

The average ultimate shear strength of the slotted simply supported channels with the free end was significantly smaller than the strength of the channels with the test setup boundary conditions. The mean value and the coefficient of variation of the V_{FEM-TS}/V_{FEM-SF} ratios were 1.69 and 0.140, respectively. The average ultimate shear strength of the slotted simply supported channels with the restrained end was reasonably close to the strength of the channels with the

test setup boundary conditions. The mean value of the $V_{FEM\text{-}TS}/V_{FEM\text{-}SF}$ ratios was 1.03 with the coefficient of variation of 0.119.

The analyses of the slotted simply supported channels with the free and restrained ends resulted in the average ultimate shear strengths that were respectively smaller and larger than the average strength of the channels with the realistic boundary conditions. The mean values and the coefficients of variations of the $V_{FEA\text{-}R}/V_{FEA\text{-}SF}$ and the $V_{FEA\text{-}R}/V_{FEA\text{-}SR}$ ratios were 1.23 and 0.159 and 0.74 and 0.093, respectively, for the slotted channels.

The obtained results show that analyses with the simplified boundary conditions with the free and restrained ends can reasonably well predict the ultimate shear strengths of the solid channels with the test setup and realistic boundary conditions. Analyses with the simplified boundary conditions with the restrained end can predict the ultimate shear strength of the slotted channels with the test setup boundary conditions with reasonable accuracy. The realistic boundary conditions of the slotted channels cannot be accurately simulated by the simply supported boundary conditions. This shows that boundary conditions affect the ultimate shear strength of the slotted channels more than the strength of the solid channels.

The ultimate shear strengths of the solid channel models C-150-0.9-1, C-200-0.9-1, and C-200-1.5-1 with all considered boundary conditions shown in Fig. 5 were higher than the elastic shear buckling loads, which indicates that the models failed in elastic or inelastic buckling and exhibited the post-buckling strength due to tension field action. The von Mises stress contours clearly show the tension field action for those models. The solid channel model CS-150-1.5-1 failed in shear yielding (see Fig. 5). It is also evident from Fig. 5 that channel models C-150-0.9-1and C-200-0.9-1 with the realistic boundary conditions failed under a combination of shear buckling and web crippling.

The slotted channel models PC-150-0.9-2, PC-200-0.9-2, and PC-200-1.5-2 with all considered boundary conditions shown in Fig. 6 failed in either elastic or inelastic buckling. They developed the post-buckling strength due to the tension field action, which can be seen in the von Mises contours in Fig. 6. The slotted channel model PCS-150-1.5-2 failed in shear yielding (see Fig. 6).

Conclusions

The effects of the boundary conditions on the elastic shear buckling loads and the ultimate shear strengths of CFS channels with solid and slotted webs were investigated numerically using non-linear finite element models developed in

ANSYS and validated against test data. The study showed that the elastic shear buckling load and the ultimate shear strength of the slotted channels are more sensitive to the boundary conditions when compared with the solid channels.

The obtained results demonstrated that the simply supported boundary conditions with the free and restrained ends can simulate the test setup boundary conditions reasonably well for the solid channels only. The analyses using the simply supported boundary conditions with the restrained end can reasonably well predict only the ultimate shear strengths of the slotted channels with the test setup boundary conditions and the solid channels with the realistic boundary conditions. Therefore, the use of the simplified boundary conditions is not recommended in the FE simulations of the test setup and realistic boundary conditions of the slotted channels and for the simulations of the realistic boundary conditions of the solid channels.

References

AISI. (2013). *AISI S310-13*, *North American Standard for the Design of Profiled Steel Diaphragm Panels*, American Iron and Steel Institute, Washington, DC.

AISI/Steel Framing Alliance. (2002a). "Development of Cost-Effective, Energy Efficient Steel Framing: Structural Performance of Slit-Web Steel Wall Studs." American Iron and Steel Institute and Steel Framing Alliance Research Report RP02-8, Washington, DC.

AISI/Steel Framing Alliance. (2002b). "Development of Cost-Effective, Energy Efficient Steel Framing: Thermal Performance of Slit-Web Steel Wall Studs." American Iron and Steel Institute and Steel Framing Alliance Research Report RP02-9, Washington, DC.

Degtyarev, V.V., and Degtyareva, N.V. (2016). "Finite element modeling of cold-formed steel channels with solid and slotted webs in shear." *Thin-Walled Structures*, 103, 183-198.

Degtyareva, N.V., and Degtyarev, V.V. (2016). "Experimental investigation of cold-formed steel channels with slotted webs in shear." *Thin-Walled Structures*, 102, 30-42.

Höglund, T., and Burstrand, H. (1998). "Slotted steel studs to reduce thermal bridges in insulated walls." *Thin-Walled Structures*, 32(1-3), 81-109.

Keerthan, P., and Mahendran, M. (2010a). "Elastic shear buckling characteristics of LiteSteel beams." *Journal of Constructional Steel Research*, 66(11),1309-1319.

Keerthan, P., and Mahendran, M. (2010b). "Experimental studies on the shear behaviour and strength of LiteSteel beams." *Engineering Structures*, 32(10), 3235-3247.

Keerthan, P., and Mahendran, M. (2015). "Improved shear design rules of cold-formed steel beams." *Engineering Structures*, 99, 603-615.

Keerthan, P., and Mahendran, M. (2014). "Improved shear design rules for lipped channel beams with web openings." *Journal of Constructional Steel Research*, 97, 127-142.

Keerthan, P., and Mahendran, M. (2011a). "New design rules for the shear strength of LiteSteel beams." *Journal of Constructional Steel Research*, 67(6), 1050-1063.
Keerthan, P., and Mahendran, M. (2013a). "New design rules for the shear strength of LiteSteel beams with web openings." *Journal of Structural Engineering*, 139, 640-656.
Keerthan, P., and Mahendran, M. (2011b). "Numerical Modeling of LiteSteel Beams Subject to Shear." *Journal of Structural Engineering*, 137(12), 1428-39.
Keerthan, P., and Mahendran, M. (2013b). "Shear buckling characteristics of cold-formed steel channel beams." *International Journal of Steel Structures*, 13(3), 385-399.
Keerthan, P., Mahendran, M., and Narsey, A. (2015). "Shear tests of hollow flange channel beams with real support conditions." *Structures*, 3, 109-119.
Kesti, J. (2000). "Local and Distortional Buckling of Perforated Steel Wall Studs," D.Sc. Dissertation, Helsinki University of Technology, Espoo, Finland.
LaBoube, R.A., and Yu, W.W. (1978). "Structural Behavior of Beam Webs Subjected Primarily to Shear Stress." University of Missouri-Rolla Final Report Civil Engineering Study 78-2, St Louis, MO.
Liptak-Varadi, J. (2010). "Equivalent thermal conductivity of steel girders with slotted webs." *Periodica Polytechnica*, 54(2), 163-170.
Pham, C.H., and Hancock, G.J. (2015). "Numerical investigation of longitudinally stiffened web channels predominantly in shear." *Thin-Walled Structures*, 86, 47-55.
Pham, C.H., and Hancock, G.J. (2010). "Numerical simulation of high strength cold-formed purlins in combined bending and shear." *Journal of Constructional Steel Research*, 66(10), 1205-1217.
Pham, C.H., and Hancock, G.J. (2012). "Tension field action for cold-formed sections in shear." *Journal of Constructional Steel Research*, 72, 168-178.
Pham, S.H., Pham, C.H., and Hancock, G.J. (2014). "Direct strength method of design for shear including sections with longitudinal web stiffeners." *Thin-Walled Structures*, 81, 19–28.
Salhab, B., and Wang, Y.C. (2008). "Equivalent thickness of cold-formed thin-walled sections with perforated webs under compression." *Thin-Walled Structures*, 46(7-8), 823-838.

Notation

$V_{cr\text{-}R}$ and $V_{cr\text{-}TS}$	elastic shear buckling loads for the realistic and test setup boundary conditions, respectively.
$V_{cr\text{-}SF}$ and $V_{cr\text{-}SR}$	elastic shear buckling load for the simply supported boundary conditions with the free and restrained ends, respectively.
$V_{FEA\text{-}R}$ and $V_{FEA\text{-}TS}$	ultimate shear strength for the realistic and test setup boundary conditions, respectively.
$V_{FEA\text{-}SF}$ and $V_{FEA\text{-}SR}$	ultimate shear strength for the simply supported boundary conditions with the free and restrained ends, respectively.
V_{test}	shear strength obtained from tests.